Clinical Science (2021) **135** 2409–2422
https://doi.org/10.1042/CS20210405

PORTLAND PRESS

Research Article

Xanthine oxidase inhibitor febuxostat reduces atrial fibrillation susceptibility by inhibition of oxidized CaMKII in Dahl salt-sensitive rats

DongZhu Xu, Nobuyuki Murakoshi, Kazuko Tajiri, Feng Duo, Yuta Okabe, Yoshiko Murakata, Zixun Yuan, Siqi Li, Kazuhiro Aonuma, Zonghu Song, Yuzuno Shimoda, Haruka Mori, Akira Sato, Akihiko Nogami, Kazutaka Aonuma and Masaki Ieda

Department of Cardiology, Faculty of Medicine, University of Tsukuba, Tsukuba, Ibaraki, Japan

Correspondence: Nobuyuki Murakoshi (n.murakoshi@md.tsukuba.ac.jp)

Oxidative stress could be a possible mechanism and a therapeutic target of atrial fibrillation (AF). However, the effects of the xanthine oxidase (XO) inhibition for AF remain to be fully elucidated. We investigated the effects of a novel XO inhibitor febuxostat on AF compared with allopurinol in hypertension rat model. Five-week-old Dahl salt-sensitive rats were fed either low-salt (LS) (0.3% NaCl) or high-salt (HS) (8% NaCl) diet. After 4 weeks of diet, HS diet rats were divided into three groups: orally administered to vehicle (HS-C), febuxostat (5 mg/kg/day) (HS-F), or allopurinol (50 mg/kg/day) (HS-A). After 4 weeks of treatment, systolic blood pressure (SBP) was significantly higher in HS-C than LS, and it was slightly but significantly decreased by treatment with each XO inhibitor. AF duration was significantly prolonged in HS-C compared with LS, and significantly suppressed in both HS-F and HS-A (LS; 5.8 $\pm$ 3.5 s, HS-C; 33.9 $\pm$ 23.7 s, HS-F; 15.0 $\pm$ 14.1 s, HS-A; 20.1 $\pm$ 11.9 s: $P<0.05$). Ca^{2+} spark frequency was obviously increased in HS-C rats and reduced in the XO inhibitor-treated rats, especially in HS-F group. Western blotting revealed that the atrial expression levels of $Met^{281/282}$-oxidized Ca^{2+}/Calmodulin-dependent kinase II (CaMKII) and Ser^{2814}-phosphorylated ryanodine receptor 2 were significantly increased in HS-C, and those were suppressed in HS-F and HS-A. Decreased expression of gap junction protein connexin 40 in HS-C was partially restored by treatment with each XO inhibitor. In conclusion, XO inhibitor febuxostat, as well as allopurinol, could reduce hypertension-related increase in AF perpetuation by restoring Ca^{2+} handling and gap junction.

Introduction

Atrial fibrillation (AF) is the most common sustained arrhythmia in clinical practice, leading to increase in mortality and morbidity, and hypertension is an evident risk factor for AF incidence [1,2]. Several lines of evidence suggest that increased production of reactive oxygen species (ROS) plays a critical role in atrial remodeling and leads to AF susceptibility [3–6]. ROS exposure in isolated myocytes and whole hearts has been shown to significantly disrupt intracellular Ca^{2+} regulation and promote a broad range of arrhythmic substrate [7–9]. Ca^{2+}/Calmodulin-dependent kinase II (CaMKII) has emerged as a compelling molecular mechanism with the potential to connect upstream proarrhythmic factors such as oxidative stress with downstream responses such as ion channel hyperactivity and defective intracellular Ca^{2+} homeostasis [10–13]. Increased ROS hyperactivates CaMKII through oxidation of methionine (Met) 281/282 on CaMKII. Elevated oxidized CaMKII (ox-CaMKII) phosphorylates Ser^{2814} on ryanodine receptor 2 (p-RyR2), causing enhanced diastolic Ca^{2+} leak from the sarcoplasmic reticulum (SR) that promotes AF. In fact, ox-CaMKII could be a biomarker and a critical proarrhythmic signal for connecting increased

Received: 23 April 2021
Revised: 06 August 2021
Accepted: 13 August 2021

Accepted Manuscript online: 13 August 2021
Version of Record published: 22 October 2021

Clinical Science (2021) **135** 2409–2422
https://doi.org/10.1042/CS20210405

atrial ROS to AF. Allopurinol is a nonspecific xanthine oxidase (XO) inhibitor [14]. Febuxostat, a relatively novel nonpurine selective inhibitor of XO, has greater bioavailability and more potent XO-inhibitory effect than allopurinol [15].

XO is a potent major enzyme producing ROS in many organs, including the heart [16–18]. XO inhibitors have been broadly used for hyperuricemia and reported to be effective for experimental model of heart failure and atherosclerosis [19,20]. However, the effect of XO inhibitors on AF remains to be fully elucidated. In the present study, we hypothesized that XO inhibitors could inhibit hypertension-related AF vulnerability through improving intracellular ROS status and ox-CaMKII signaling pathway. We aimed to investigate the effects of a nonpurine selective XO inhibitor febuxostat, compared with a purine analog allopurinol, in an *in vivo* hypertension rat model.

Methods

Animal model and physiological study

After receiving approval from the Institutional Animal Experiment Committee of the University of Tsukuba, animal experiments were carried out humanely and in accordance with the Guide for the Care and Use of Laboratory Animals published by the U.S. National Institutes of Health (NIH Publication No. 85-23, revised 1996), the Regulation for Animal Experiments in our university, and the Fundamental Guidelines for Proper Conduct of Animal Experiment and Related Activities in Academic Research Institutions under the jurisdiction of the Ministry of Education, Culture, Sports, Science and Technology of Japan.

Male five-week-old Dahl salt-sensitive rats were fed either 0.3% NaCl (low-salt; LS) or 8% NaCl (high-salt; HS) diet. After 4-weeks of diet, HS diet rats were divided into three groups: the test drugs were administered ally using a nasogastric tube (KN-349, Natsume, Tokyo, Japan) to vehicle (HS-C) (0.4% methylcellulose, 0.5 ml/day), febuxostat (HS-F) (5 mg/kg/day [21], a kind gift from Teijin Pharma Ltd., Tokyo, Japan), or allopurinol (HS-A) (50 mg/kg/day [26,27]). All the animals were randomly assigned to each group. After 8 weeks of diet and 4 weeks of treatment, systolic and diastolic blood pressures were measured by blood pressure measurement system for small animals, BP-98A-L (Softron, Tokyo, Japan). The averages of five times measurements in each rat were accepted. After that, cardiac function was analyzed under anesthesia with isoflurane by echocardiography, Vevo 2100 (Visual Sonics, Toronto, Canada). Forty-eight rats (n=12 per each group) underwent AF induction and electrophysiological study only. The other 48 rats were used to obtain biochemical and histological data without AF induction to avoid causing catheter-related mechanical effects in the biochemical and histological analyses. The atria were harvested and quickly frozen with liquid nitrogen for assessment of the atrial expression of mRNA and protein or were preserved with a fixative for histological examination.

Electrophysiological study and AF induction study

AF induction study protocol was described in our previous report [22]. Briefly, a right cervical vein cut-down was performed, and a 2-Fr quadripolar electrode catheter with 2-mm distance (Ensemble; Japan Lifeline Co., Ltd., Tokyo, Japan) was inserted into the right atrium under anesthesia. The catheter was placed at the site where the amplitude of the intraatrial electrogram was higher than that of the intraventricular electrogram (Figure 1A,B). To measure the atrial muscle effective refractory period (AEPR), a programmable stimulator (SEN-7203; Nihon Kohden, Tokyo, Japan) was used to deliver approximately measured at basic cycle lengths (CLs) of 150, 120, and 100 ms with a train of 8 basic stimuli (S1 × 8) followed by a single extrastimulus (S2) at 5-ms decrements. AERP was defined as the longest S1–S2 interval that failed to capture. To induce AF, atrial burst pacing was delivered through two poles of the electrode catheter by a programmable stimulator at an amplitude of 6 Volts, CL of 20 ms, pulse duration of 6 ms, and stimulation time of 30 s. Atrial burst pacing was performed five times in each rat. Inducible rate was determined by calculating the number of AF episodes divided by the number of total procedures. AF duration was defined as the interval between initiation and spontaneous termination of AF. We averaged the duration of AF with five-time inductions in each group.

Confocal calcium imaging

Atrial cardiomyocytes were isolated from LS, HL-C, HS-F, HS-A rats using a Langendorff-free procedure [20,21]. The isolated cells were incubated with Fluo-4 AM (Invitrogen, Carlsbad, CA, U.S.A.) diluted in 20% Pluronic F-127 DMSO at 5 μM final concentration in Tyrode buffer (NaCl, 140 mM, KCl 5 mM, HEPES 5 mM, NaH_2PO_4 2 mM, $MgCl_2$ 1 mM, glucose 10 mM, pH 7.4) for 10 min, Tyrode's solution with 1.8 mM Ca^{2+}. The cells were then rinsed with Tyrode buffer and maintained in the buffer during experiments. To capture the Fluo-4 AM signals, live cell imaging was performed with a 40× lens on Leica TCS SP8 LSCM Confocal Microscope System (Leica Microsystems,

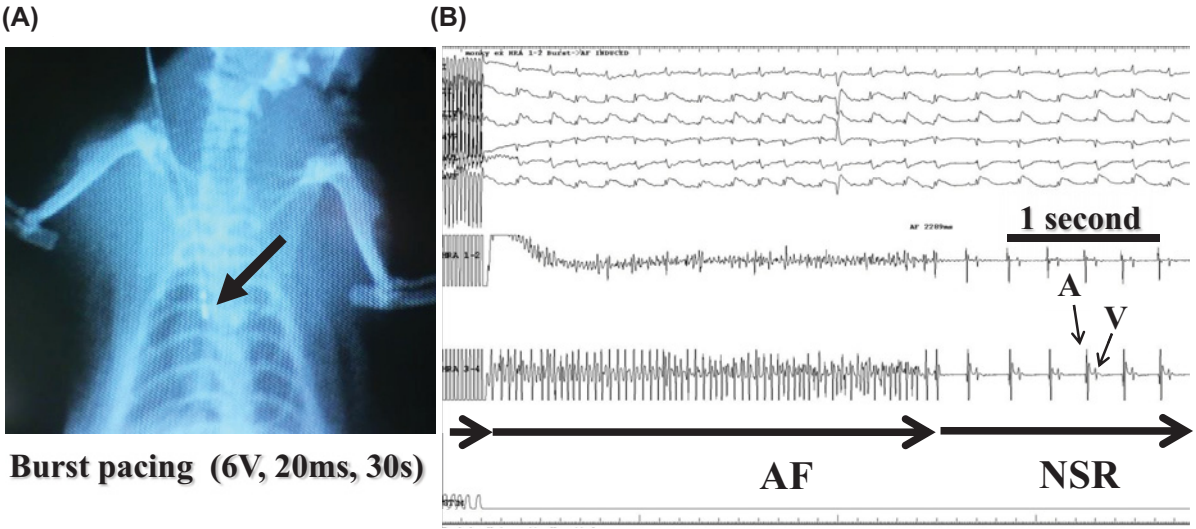

Figure 1. AF induction study

(**A**) X-ray photograph showed that 2-Fr catheter reached at the right atria (arrow). (**B**) Upper six lanes showed typical recordings of limb-leads of surface electrocardiograms. Middle lane showed endocardial electrocardiogram placed at mid-right atrium, and bottom lane showed endocardial electrocardiogram placed at high right atrium during induced AF, followed by spontaneous termination to normal sinus rhythm (NSR).

Wetzlar, Germany). Line scan images were recorded along the cell's longitudinal axis at 500 Hz, with a pixel size of 100 nm and pinhole optimized for a resolution of 0.4 μm in the focal plane and <1 μm in the z-axis. Isoproterenol (Iso) was added to the cell after the baseline was established. Baseline fluorescence (F_0) was determined by averaging ten images without calcium spark activity. Fractional fluorescence increases (F/F_0) were determined in areas (2.2 × 2.2 μm) where calcium sparks were detected. Calcium sparks were defined as local fractional fluorescence increases >1.3. Calcium sparks were detected and characterized following established criteria [23,24]. To evaluate calcium sparks, cytoplasmic fluorescence signals were obtained using LAS-X software (Leica Microsystems) and ImageJ version 1.45 software (n=10 in LS group, n=8 in HS-C group, n=8 HS-F group, n=7 in HS-A group).

RNA isolation and real-time RT-PCR

RNA isolation and real-time RT-PCR were performed according to the methods described in our previous papers [25]. Briefly, total RNA was isolated from the excised left atrium (LA) with TRIzol (Thermo Fisher, MA, U.S.A.). Total RNA (1 μg) was reverse transcribed using a Ready-To-Go T-Primed First-Strand Kit (GE Healthcare UK Ltd., Buckinghamshire, England) first-strand cDNA synthesis. Detection of mRNA expression levels was performed by real-time quantitative RT-PCR with ABI Prism 7500 Sequence Detector System (Thermo Fisher). For each assay, 10 ng of the cDNA were mixed with 12.5 μl of TaqMan Universal PCR Master Mix and 1.25 μl of TaqMan primer and probe (Thermo Fisher). Fold-change analysis was based on standardizing RNA levels by correcting for 18S RNA levels in the sample. Assay IDs of TaqMan primers and probes used in the present study were as follows: *Ryr2* (Rn01470303_m1), *CamkIId* (Rn00560913_m1), *Serca2a* (Rn00568762_m1), *Pln* (Rn01434045_m1), *Il1r2* (Rn00588589_m1), *Il6* (Rn01410330_ml), *Tgfb* (Rn99999016_ml), $p22^{phox}$ (Rn00577357_m1), and *18S rRNA* (Hs99999901_s1). The result for each gene was obtained from three independent measurements (n=4 per group) performed in duplicate.

Western blot analysis

Western blotting was performed in according with the methods described in our previous papers [22]. Briefly, isolated left atria were homogenized in the lysis buffer including PRO-PREP protein extraction kit (iNtRON Biotechnology, INC., Daejoen, Korea). After centrifugation (8000×g, 10 min, 4°C), the supernatants were used for Western immunoblotting. Appropriate volumes of the samples (30 μg/lane) were mixed with an equal volume of sample buffer, heated at 95°C for 5 min, and then subjected to SDS/PAGE using polyacrylamide gels. The proteins were transferred by semidry electroblotting from gels to polyvinylidene difluoride membranes. The blots were then blocked with the

Clinical Science (2021) **135** 2409–2422
https://doi.org/10.1042/CS20210405

primary antibodies, CaMKII (1:1000, Abcam, Cat No. ab32678), Ox-CaMKII polyclonal antibody (1:1000, Merck Millipore, Darmstadt, Germany, Cat No. 07-1496), RyR2 (1:2000, Badrilla, Cat No. A01013), Ser^{2814}-phosphorylated RyR2 (p-RyR2) (1:2000, Badrilla, Cat No. A010-31AP), SERCA2a (1:10000, Abcam, Cat No. ab150435), phosphorylated SERCA2a (p-SERCA2a) (1:1000, Thermo Fisher, MA3-919)], phospholamban (PLB) (1:1000, Abcam, Cat No. ab15000), and phosphorylated PLB (p-PLB) (1:5000, Badrilla, Cat No. A010-13) for several hours at 4°C. Next, the blots were incubated with an appropriate second antibody, horseradish peroxidase-conjugated goat anti-rabbit IgG (Cell Signaling Technology). Immunoreactions were visualized with an enhanced chemiluminescence method. Densitometric analysis was performed on scanned immunoblot images with the ImageJ gel analysis tool (Ver. 1.42q, NIH, U.S.A.). The result of each ratio of examined protein/tubulin protein was obtained from two independent measurements.

Measurement of myocardial XO activity

Cayman's Xanthine Oxidase Fluorometric Assay Kit (Cayman Chemical, Ann Arbor, Michigan, U.S.A.) was used to measure myocardial tissue XO activity. Atrial tissues were excised, rinsed with PBS, and homogenated. After centrifugation, 50 μl of supernatants were applied to a 96-well plate, and assay cocktail was mixed. After 45-min incubation at 37°C, XO activity was measured using an excitation wavelength of 520–550 nm and an emission wavelength of 585–595 nm by Varioskan System (Thermo Fisher).

Histological analysis

Atrial samples from the LA free wall were immersed in 4% paraformaldehyde in PBS for more than 24 h, embedded in paraffin, and sliced into 4-μm-thick sections. Sections were stained with Masson's Trichrome. We randomly selected 12 sections from six rats per group and evaluated them at 100-fold magnification. Fibrous tissue was quantified with SigmaScan 4.0 (Jandel Scientific, San Rafael, CA, U.S.A.). The blue pixel content of digitized images was detected as interstitial fibrotic area and measured relative to total tissue area with a digital imaging analyzer (Scion Image 4.0.3; Scion Corporation, Frederick, MD, U.S.A.).

Immunofluorescence

To evaluate the expression of connexin 40, we performed immunofluorescence. In brief, sections after antigen retrieval were incubated with rabbit polyclonal anti-connexin 40 antibody (1:500; Cell Signaling Technology, Danvers, MA, U.S.A.) followed by treatment with AlexaFluora-488 goat anti-rabbit IgG (1:500; Thermo Fisher) as a secondary antibody. The sections were investigated and captured by BZ-X700 (Keyence, Osaka, Japan).

Statistical analysis

Data are expressed as means ± SEM. All parameters were compared by one-way analysis of variance (ANOVA), followed by Tukey–Kramer post-hoc test. A value of $P<0.05$ denoted the presence of a statistically significant difference.

Results

Physiological findings of hypertensive rat model

Systolic blood pressure (SBP) was progressively elevated in HS groups at 9 and 13 weeks of age compared with that at 5 weeks of age baseline. SBP was also significantly higher in HS-C group than LS group at 13 weeks of age, and it was significantly decreased in both HS-F and HS-A groups (Table 1).

Echocardiographic parameters are also shown in Table 1. Left ventricular diastolic diameter (LVDd) and left ventricular systolic diameter (LVDs) were gradually increased in all groups. At 13 weeks of age, LVDd and LVDs were significantly larger, and ejection fraction (EF) was significantly lower in all HS groups than in LS group. EF was slightly improved by each XO inhibitor but not significantly different between all HS groups (Table 1). Left atrial diameter (LAD) was significantly larger in HS-C groups than in LS group at 9 weeks of age and more enlarged at 13 weeks. It was tended to be decreased in both treated groups compared with HS-C; however, there was also no significant difference between all HS groups (Table 1). The ratios of atrial weight/body weight and left ventricular (LV) weight/body weight was significantly increased in all HS groups compared with LS, suggesting that atrial and LV hypertrophy occurred in Dahl salt-sensitive rats with HS diet at 13 weeks of age (Figure 2A,B). However, there were no significant differences between HS-C, HS-F, and HS-A groups.

Table 1 Blood pressure and echocardiographic parameters

	LS (*n*=12)	HS-C (*n*=12)	HS-F (*n*=12)	HS-A (*n*=12)
SBP (mm/Hg)				
5 weeks	105.4 ± 13.2	105.0 ± 2.8	104.2 ± 8.4	106.3 ± 8.1
9 weeks	122.2 ± 13.6‡	165.0 ± 18.9*‡	165.8 ± 16.4*‡	167.7 ± 22.5*‡
13 weeks	128.8 ± 10.5‡	186.4 ± 11.9*‡§	169.5 ± 11.2*†‡	173.6 ± 9.0*†‡§
LVDd (mm)				
5 weeks	5.73 ± 0.55	5.92 ± 0.38	5.65 ± 0.53	5.84 ± 0.45
9 weeks	7.34 ± 0.53‡	7.31 ± 0.40‡	7.40 ± 0.35‡	7.25 ± 0.41‡
13 weeks	7.42 ± 0.73‡	7.86 ± 0.94*‡	8.03 ± 0.52*‡	7.95 ± 0.76*‡
LVDs (mm)				
5 weeks	3.30 ± 0.34	3.67 ± 0.35	3.43 ± 0.44	3.60 ± 0.49
9 weeks	4.53 ± 0.30‡	5.07 ± 0.60*‡	4.37 ± 0.65†‡	4.24 ± 0.21†‡
13 weeks	4.63 ± 0.62‡	5.45 ± 0.84*‡	5.69 ± 0.62*‡	5.76 ± 0.76*‡
FS (%)				
5 weeks	42.23 ± 5.34	43.07 ± 5.96	39.29 ± 3.67	40.47 ± 6.35
9 weeks	38.28 ± 0.36	30.69 ± 4.67*‡	41.18 ± 6.30†‡	37.71 ± 3.37†‡
13 weeks	37.81 ± 2.75‡	30.84 ± 3.75*‡	29.18 ± 4.91*‡§	27.71 ± 4.07*‡§
EF (%)				
5 weeks	70.3 ± 6.5	67.7 ± 5.5	69.0 ± 4.5	69.9 ± 7.6
9 weeks	66.9 ± 3.2	56.7 ± 6.8*‡	70.1 ± 7.8†	66.4 ± 4.3†‡
13 weeks	66.3 ± 3.7	50.7 ± 2.1*‡§	53.9 ± 2.0*‡§	51.9 ± 4.1*‡§
LAD (mm)				
5 weeks	3.36 ± 0.24	3.38 ± 0.17	3.22 ± 0.28	3.26 ± 0.31
9 weeks	4.10 ± 0.17‡	4.28 ± 0.22‡	4.26 ± 0.20‡	4.37 ± 0.72‡
13 weeks	4.22 ± 0.21‡	5.83 ± 0.53*‡§	5.49 ± 0.37*‡§	5.34 ± 0.29*‡§

Data are expressed as mean ± SD. Abbreviations: EF, ejection fraction; LAD, left atrial dimension; LVDd, left ventricular diastolic diameter; LVDs, left ventricular systolic dimension; LVFS, left ventricular fractional shortening. *n*=12 in each group.
*P<0.05 vs. LS.
†P<0.05 vs. HS-C.
‡P<0.05 vs. 5 weeks.
§P<0.05 vs. 9 weeks.

Table 2 Electrophysiological parameters

	LS (*n*=12)	HS-C (*n*=12)	HS-F (*n*=12)	HS-A (*n*=12)
Mean AF time (s)	5.8 ± 3.5	33.9 ± 23.7*	15.0 ± 14.1*†	20.1 ± 11.9*†
AERP				
CL150 ms	77.0 ± 2.6	70.3 ± 2.6*	75.0 ± 2.8†	74.7 ± 4.5*†
CL120 ms	77.0 ± 1.7	71.3 ± 3.1*	76.5 ± 2.7†	75.3 ± 3.5*
CL100 ms	76.7 ± 2.5	71.7 ± 2.5*	76.5 ± 1.7†	72.3 ± 3.2†

Data are expressed as mean ± SD. *n*=12 in each group.
*P<0.05 vs. LS.
†P<0.05 vs. HS-C.

Electrophysiological study and AF induction

After 4-week treatment, we performed the electrophysiological study and AF induction. The basal heart rate was not significantly different between LS and all HS groups. The AERPs were significantly shortened in HS-C group than in LS group at CLs of 150, 120, and 100 ms, and those were restored by treatment with febuxostat in each CL, whereas those were restored by treatment with allopurinol only at CL of 150 and 120 ms (Table 2). After 30-s burst pacing, AF was reproducibly induced in each group, followed by spontaneous termination (Figure 1B). There was no significant difference in inducible rate between all groups (inducible rate LS 90.0%; HS-C 97.6%; HS-F 87%; HS-A 90%). However, mean AF duration was significantly prolonged in HS-C group compared with LS group, and it was significantly shortened by treatment with both febuxostat and allopurinol (LS, 5.8 ± 3.5 s; HS-C, 33.9 ± 23.7 s; HS-F, 15.0 ± 14.1 s; HS-A, 20.1 ± 11.9 s; P<0.05) (Figure 2C). We further investigated XO activity in the atria of each

Clinical Science (2021) **135** 2409–2422
https://doi.org/10.1042/CS20210405

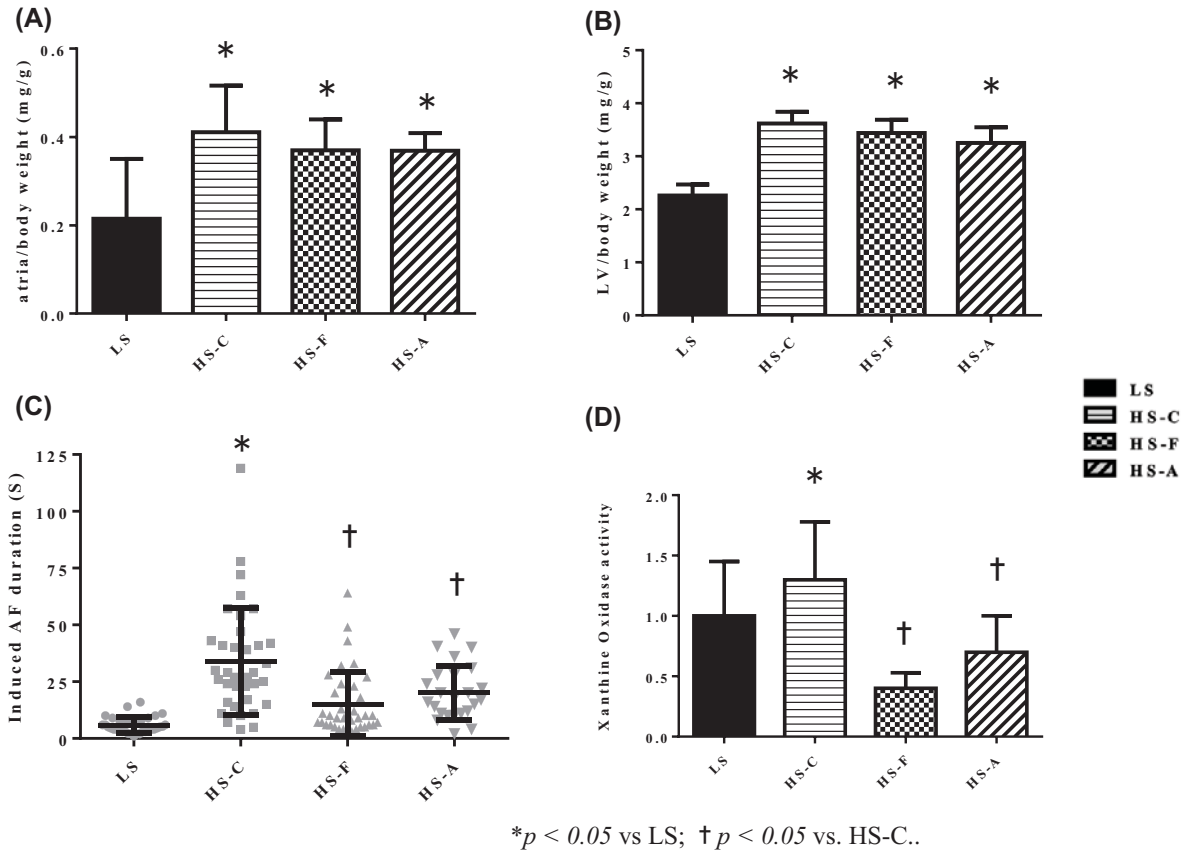

Figure 2. Tissue weight per body weight, AF duration, and XO activity

(**A**) At 13 weeks of age, the ratio of atrial tissue weight to body weight was significantly higher in HS-C than LC, and it was not significantly different among HS-C, HS-F, and HS-A (LS: 0.22 ± 0.14; HS-C: 0.41 ± 0.11; HS-F: 0.37 ± 0.07; HS-A: 0.37 ± 0.04; n=12 in each group). (**B**) At 13 weeks of age, the ratio of LV weight to body weight was significantly higher in HS-C than LC, and it was not significantly different between all HS-groups (LS: 2.26 ± 0.21, HS-C: 3.62 ± 0.22, HS-F: 3.44 ± 0.25, HA-A: 3.25 ± 0.30, n=12 in each group). (**C**) Mean AF duration was significantly prolonged in HS-C compared with LS, and it was significantly suppressed by each XO inhibitor (LS: 5.8 ± 3.5 s; HS-C: 33.9 ± 23.7 s; and 20.1 ± 11.9 s; HS-A: 15.0 ± 14.1 s, n=12 in each group). *P<0.05 vs. LS; †P<0.05 vs. HS-C. (**D**) XO activity was significantly higher in the HS versus the LS rats by 1.3-fold, and it was significantly reduced in the HS-F and HS-A. *P<0.05 vs LS; †P<0.05 vs. HS-C (n=5, in each group).

group. XO activity in the atrial tissue was significantly higher in HS-C group versus LS group, and it was significantly reduced in the XO inhibitor-treated rats, especially in HS-F group (Figure 2D).

Intracellular Ca^{2+} imaging and analysis

Representative confocal microscopy line-scan images of atrial cardiomyocytes to evaluate Ca^{2+} sparks with isoproterenol stimulation are shown in Figure 3. Under β-receptor stimulation, Ca^{2+} sparks and mini waves were clearly increased in HS-C, and were reduced by the treatment with each XO inhibitor (Figure 3A). The Ca^{2+} fluorescence ratio (F/F_0) and Ca^{2+} spark frequency (sparks/scan) were significantly increased in HS-C rats and significantly reduced in the XO inhibitor-treated rats, especially in HS-F group (Figure 3B,C).

Expression of AF-related molecules

We investigated the expression levels of AF-related genes by quantitative real-time RT-PCR in the atrial tissue. The mRNA expression levels of calcium handling-related genes, *Ryr2*, *Serca2a*, and *CamkII*, were significantly increased in HS-C compared with LS, and those were significantly decreased in HS-F (Figure 4A). On the other hand, the expression level of *Pln* mRNA was not altered between all groups. The mRNA expression levels of *Tgfb* and $p22^{phox}$,

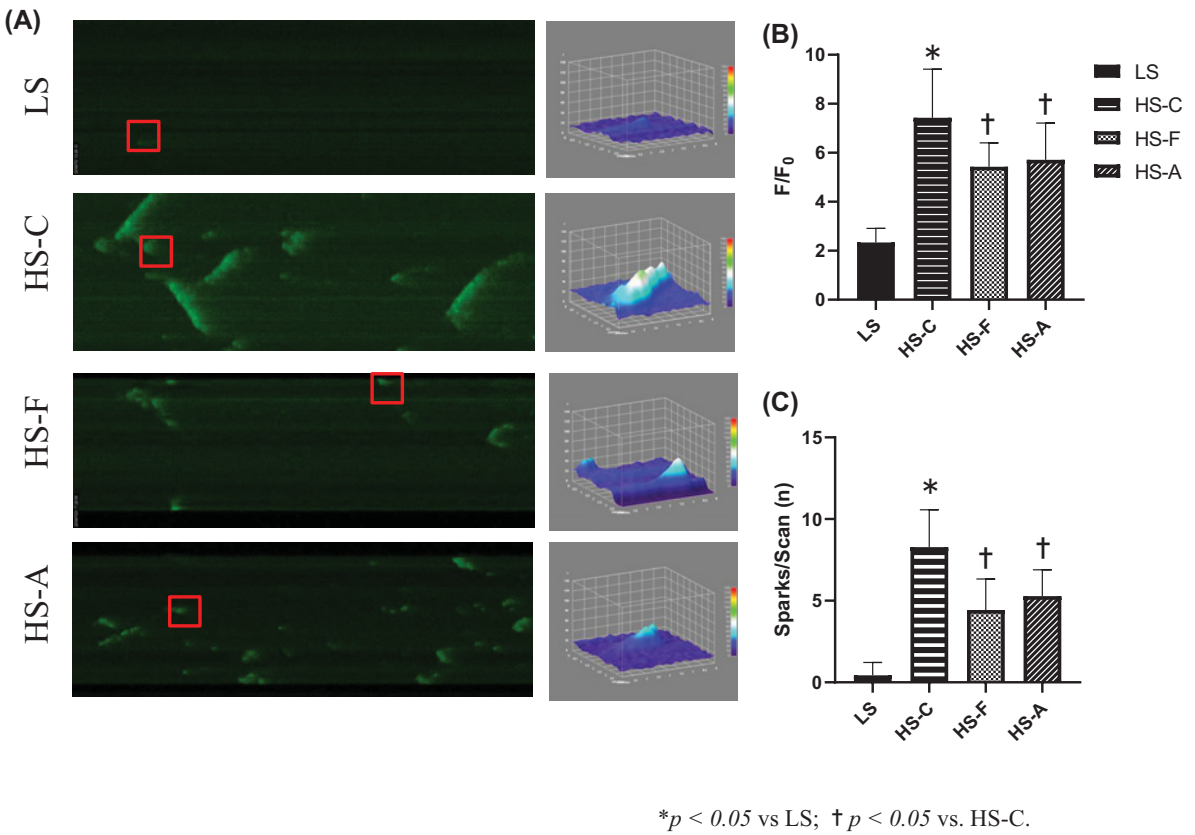

$^{*}p < 0.05$ vs LS; † $p < 0.05$ vs. HS-C.

Figure 3. Calcium imaging of isolated cardiomyocytes

(**A**) Representative calcium images of isolated cardiomyocytes obtained by confocal microscopy (left panel), and representative images of 3D surface plot of calcium sparks of each groups (right panel). (**B**) Scatter chart fractional fluorescence increases (F/F_0) (LS: 2.12 ± 0.62; HS-C: 7.31 ± 1.41; HS-F: 5.73 ± 0.67; HS-A: 5.87 ± 0.92). *$P<0.05$ vs LS; †$P<0.05$ vs. HS-C. (**C**) Numbers of calcium sparks and mini waves per scan. Mini waves are defined as the calcium waves which did not transport throughout the cardiomyocyte, but only a portion of the cell (LS: 1.00 ± 0.73; HS-C: 7.35 ± 2.14; HS-F: 4.36 ± 1.78; HS-A: 4.87 ± 1.42). *$P<0.05$ vs LS; †$P<0.05$ vs. HS-C.

NADPH oxidase subunit, were also significantly increased in HS-C compared with LS, and those were significantly decreased in HS-F (Figure 4B). On the other hand, the inflammatory cytokine-related mRNA expression levels of *Il6* were not significantly different among the four groups. *Il1r2* significantly increased in HS-C group, and decreased in allopurinol-treated group but not statistically significant, and did not change on treatment with febuxostat.

Next, we evaluated the expression levels of calcium handling-related proteins by Western blotting in the atrial tissue (Figure 5). The ratio of ox-CaMKII to total CaMKII was significantly increased in HS-C, and it was significantly reduced by each XO inhibitor. Likewise, the ratio of p-RyR2 to total RyR2 and the ratio of p-SERCA2a to total SERCA2a was also significantly increased in HS-C rats and significantly reduced by each XO inhibitor, especially febuxostat. On the other hand, p-PLB and PLB expression levels were not significantly different among the four groups.

Fibrosis and immunofluorescence of connexin 40 in the atrial tissues

Histological analysis revealed that interstitial fibrosis occurred to a greater degree in the atrial section of HS-C versus LS, and the amounts of fibrosis in the atrial sections of both HS+F and HS+A were reduced (Figure 6A). We further investigated the expression level of gap junction protein connexin 40 by immunofluorescence (Figure 6B). Compared with LS, the atrial tissue from HS-C displayed weaker immunofluorescence intensity of connexin 40, whereas it was partially restored by each XO inhibitor. Distribution pattern of connexin 40 was disarranged in HS-C rats, and it was partially improved by febuxostat or allopurinol treatment.

Clinical Science (2021) **135** 2409–2422
https://doi.org/10.1042/CS20210405

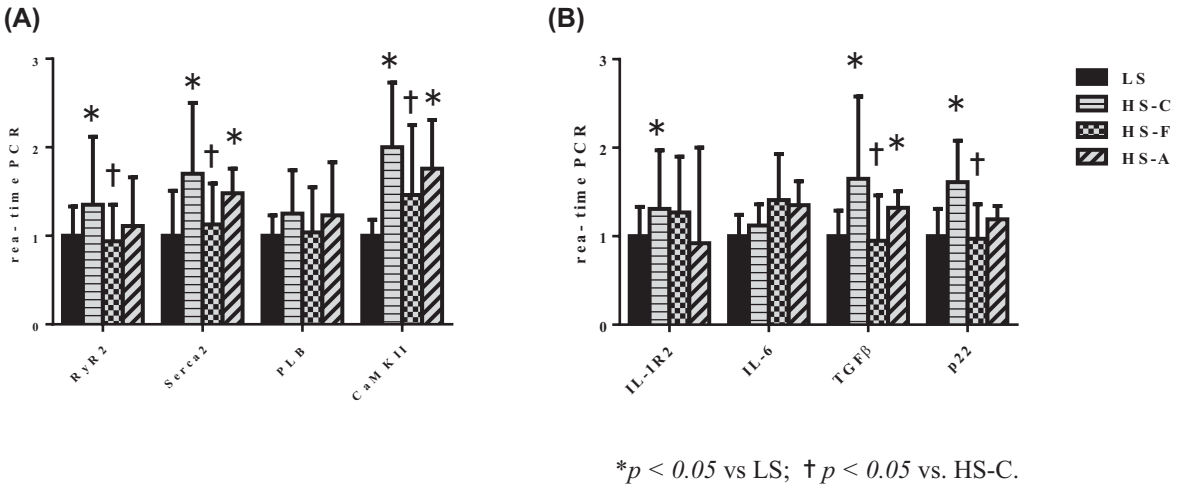

Figure 4. mRNA expression analysis by real-time PCR

(**A**) The mRNA expression levels of calcium handling-related genes *Ryr2*, *Serca2a*, *CamkII* in the atrial tissues were significantly increased in HS-C compared with LS, and those were significantly decreased by treatment with febuxostat. The expression level of *Pln* was not significantly altered between all groups (Ryr2; LS: 1.00 ± 0.52; HS-C: 1.69 ± 0.80; HS-F: 1.33 ± 0.46; HS-A: 1.48 ± 0.28) (Serca2; LS: 1.00 ± 0.73; HS-C: 7.35 ± 2.14; HS-F: 4.36 ± 1.78; HS-A: 4.87 ± 1.42) (Pln; LS: 1.00 ± 0.23; HS-C: 1.25 ± 0.49; HS-F: 1.05 ± 0.51; HS-A: 1.23 ± 0.60) (CamkII; LS: 1.00 ± 17, HS-C: 2.00 ± 0.74; HS-F: 1.46 ± 0.79; HS-A: 1.76 ± 0.55). **P*<*0.05* vs LS; †*P*<*0.05* vs. HS-C. *n*=4 in each group. (**B**) The mRNA expression levels of *Tgfb* and $p22^{phox}$, NADPH oxidase subunit, were significantly increased in HS-C compared with LS, and those were significantly decreased in HS-F. The inflammatory cytokine-related mRNA expression levels (*Il1r2* and *Il6*) were not significantly different among the four groups (*Il1r2*; LS: 1.00 ± 0.33; HS-C: 1.31 ± 0.66; HS-F: 1.27 ± 0.63; HS-A: 0.92 ± 1.08) (*Il6*; LS: 1.00 ± 0.24; HS-C: 1.11 ± 0.24; HS-F: 1.42 ± 0.52; HS-A: 1.35 ± 0.27) (*Tgfb*; LS: 1.00 ± 0.29; HS-C: 1.65 ± 0.93; HS-F: 0.95 ± 0.51; HS-A: 1.31 ± 0.18) ($p22^{phox}$; LS: 1.00 ± 0.31; HS-C: 1.61 ± 0.47; HS-F: 0.97 ± 0.39; HS-A: 1.19 ± 0.15). **P*<*0.05* vs LS; †*P*<*0.05* vs. HS-C. *n*=4 in each group.

Discussion

Previous studies reported that each febuxostat or allopurinol prevented atrial remodeling and reduced AF vulnerability in atrial tachypacing-induced heart failure canine model [26–28]. In this study, we showed that both XO inhibitors febuxostat and allopurinol significantly suppressed hypertension-related atrial remodeling and AF perpetuation via restoring CaMKII oxidization and RyR2 hyperphosphorylation. Our study showed a class effect of XO inhibitors and a novel mechanism of suppressing AF by XO inhibitors.

Previous studies reported that electrical remodeling occurred in the atria from Dahl salt-sensitive rats fed to HS diet, shown as shortening of AERP [29,30]. ERP shortening makes re-entry more likely to keep rotating in the atria and leads to AF perpetuation. In the present study, we confirmed a shorter AERP and a longer AF duration in HS group than LS group, suggesting that arrhythmogenic substrate has been formed in the atria from Dahl salt-sensitive rats fed to HS diet. The present study also demonstrated that hypertension-related increase in atrial XO activity was significantly reduced by febuxostat and allopurinol. Oxidative stress strongly contributes to the development of arrhythmogenic atrial remodeling [3,4,31,32]. NADPH oxidase and XO activities have been reported to be increased in the fibrillating atria and considered as major sources of AF-related increase in ROS [4]. XO activity has been correlated with oxidative stress and elevation of systemic inflammatory markers [33]. Both XO inhibitors were suggested to sufficiently suppress the XO-derived oxidative stress in the atrial tissues, consequently contributing to the suppression of arrhythmogenic electrical remodeling.

Previous studies indicated important cross-talks between XO and NADPH oxidase, and between XO and neuronal nitric oxide synthase (nNOS), both major sources of ROS in the diseased heart. ROS derived from the NADPH oxidase can increase conversion of xanthine dehydrogenase into XO [26], and hydrogen peroxide (H_2O_2) produced from XO can stimulate NADPH oxidase [4]. In addition, XO-derived ROS increases NADPH oxidase activity, and inhibition of XO activity either by allopurinol or by siRNA prevented NADPH activation. Moreover, deficiency of nNOS leads to profound increases in XO-mediated O_2 production, which in turn depresses myocardial excitation–contraction coupling in a manner reversible by XO inhibition with allopurinol [17,33]. Therefore, atrial increase in ROS may be

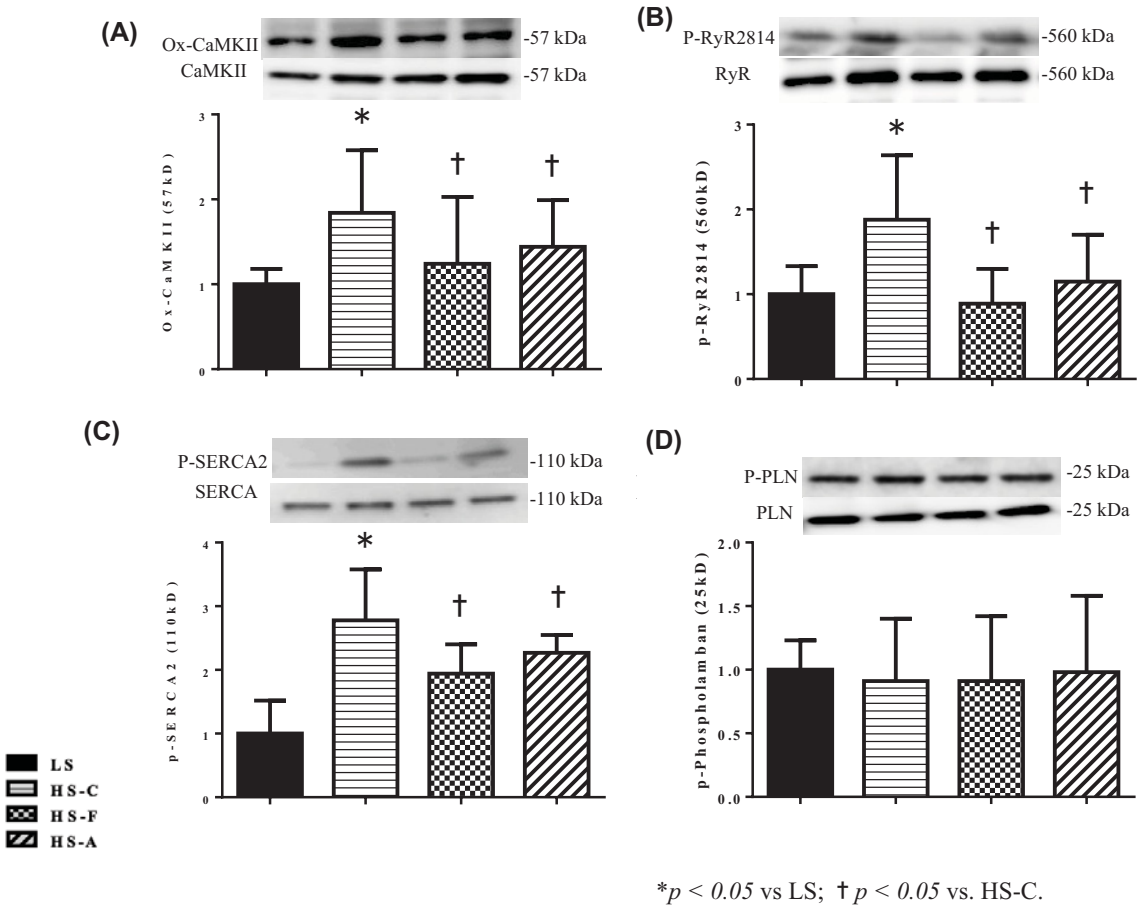

Figure 5. Protein expression analysis by Western blotting

(**A**) The ratio of ox-CaMKII to total CaMKII was significantly increased in HS, and significantly reduced by XO inhibitors (ox–CaMKII/CaMKII; LS: 1.00 ± 0.18; HS-C: 1.84 ± 0.74; HS-F: 1.24 ± 0.79; HS-A: 1.44 ± 0.65). (**B**) Likewise, the ratio of Ser^{2814}-phosphorylated RyR2 to total RyR2 was also significantly increased in HS rats, and significantly reduced by XO inhibitors (p-RyR2/RyR; LS: 1.00 ± 0.33; HS-C: 1.84 ± 0.76; HS-F: 1.23 ± 0.41; HS-A: 1.35 ± 0.565). (**C**) The ratio of phosphorylated SERCA2 to total SERCA2 was significantly increased in HS, and significantly reduced by XO inhibitors (p-SERCA2/SERCA; LS: 1.00 ± 0.52; HS-C: 2.79 ± 0.80; HS-F: 1.94 ± 0.46; HS-A: 2.27 ± 0.28). (**D**) The ratio of phosphorylated PLN to total PLN was not significantly different among the four groups (p-PLN/PLN; LS: 1.00 ± 0.23; HS-C: 0.91 ± 0.49; HS-F: 0.91 ± 0.51; HS-A: 0.98 ± 0.60). *$P<0.05$ vs. LS; †$P<0.05$ vs. HS-C. n=4 in each group.

the result of interaction between XO and other sources of ROS such as NADHP oxidase and nNOS, and the inhibitory effect of XO inhibitors on AF may be at least partly due to its indirect interruption with NADPH oxidase and/or nNOS pathway.

There is growing evidence that increased oxidative stress linked to intracellular Ca^{2+} handling in the pathophysiology of AF [4–6,34,35]. CaMKII plays an important role in conducting the frequency and amplitude intracellular Ca^{2+} transients [36] and can also be a critical ROS sensor for transducing increased ROS to AF susceptibility [11]. CaMKII is hyperactivated by an angiotensin II (Ang II)- and aldosterone-dependent increase in ROS through oxidation of methionine (Met) 281/282 CaMKII. Ser^{2814} on RyR2 is a validated ox-CaMKII phosphorylation target, and phosphorylation of its site promotes diastolic sarcoplasmic reticulum Ca^{2+} leak, which triggers delayed after depolarizations that promotes AF [37]. In this study, we showed that $Met^{281/282}$-ox-CaMKII and Ser^{2814}-phosphorylated RyR2 expressions were significantly enhanced in the atria from Dahl salt-sensitive rats with HS diet, and those were significantly suppressed by 4-week treatment with XO inhibitors. Favorable effect of XO inhibitors on hypertension-related AF could be accounted for restoring intracellular Ca^{2+} handling through modification of ox-CaMKII-phosphorylated RyR2 pathway. Also, we demonstrated by calcium imaging that XO inhibitors decreased Ca^{2+} sparks and mini waves

Clinical Science (2021) **135** 2409–2422
https://doi.org/10.1042/CS20210405

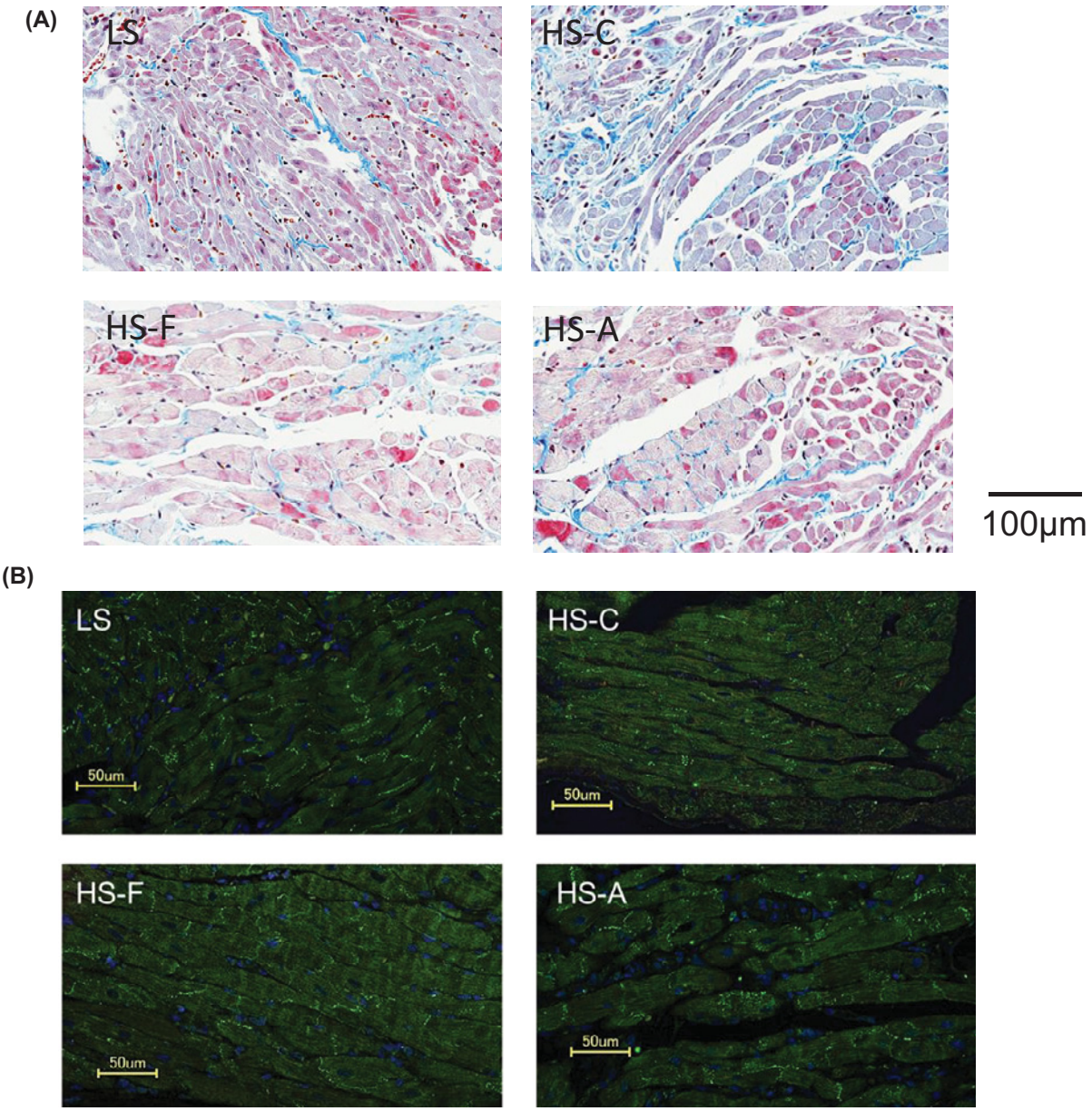

Figure 6. Histology and immunofluorescence for connexin 40 in the atrial tissues

(**A**) Representative images of Masson's Trichrome staining. Interstitial fibrosis was observed to a greater degree in the atrial section of HS-C than LS, and the amounts of fibrosis in both HS -F and HS-A were reduced. *n*=5 in each group. (**B**) Representative images of immunofluorescence for connexin 40. Fluorescence intensity of connexin 40 was decreased in HS group, and improved by XO inhibitors. Distribution pattern of connexin 40 was disarranged in HS group, but partially restored by febuxostat and allopurinol treatment. *n*=5 in each group.

in HS-C. The frequencies of Ca^{2+} sparks and mini waves measured by confocal microscopy are directly correlated with diastolic SR Ca^{2+} leaks, suggesting that XO inhibitors could reduce AF perpetuation through suppressing diastolic Ca^{2+} leaks from SR.

Moreover, it has been reported that activated CaMKII can also phosphorylate L-type Ca channel (Cav1.2) and Na channel (Nav1.5). The former increases L-type Ca^{2+} current, shortens AERP and causes early after depolarizations (EADs), and the latter is likely to shift their availability to more negative membrane potentials but also enhances the long-lasting late sodium current favoring EADs [10]. Therefore, XO inhibitors may exert a reversal effect on the

hypertension-related electrical remodeling of the other channels such as L-type Ca^{2+} channel or Na channel through suppressing CaMKII hyperactivation.

Atrial inflammation and fibrosis are also important pathogenesis of AF, especially with respect to electrical conduction disturbance, and fibroblast ion channels abnormality involving in Ca^{2+} entry pathways. These increase the heterogeneity of impulse propagation and enhance atrial re-entry, which be directly related to the mechanisms responsible for initiating and maintaining AF [38]. Recent studies demonstrated that atrial fibrogenesis in patients with AF is associated with changes in TGF-β1 [39]. In this study, structural remodeling due to interstitial fibrosis has been observed, and the mRNA expression of *Tgfb* significantly increase in the HS-C rats, and reversed by treatment with XO inhibitor, which eventually leads to a reduction in atrial fibrosis.

Connexin 40 is a major gap-junction protein in the atrial myocardium. Conduction disturbance is caused by impaired either cell-to-cell coupling via electrical remodeling of gap junction channels and voltage-gated Na channel or side-to-side electrical coupling via structural remodeling of extracellular matrix and fibrosis [40]. The distribution and amount of gap junctions may influence the electrical conduction properties [41], and abnormal Cx40 expression is involved in both trigger formation and enhanced vulnerability of the atrial myocardium to AF [42]. This study showed that gap junction Cx40 expression was decreased, and heterogeneously distributed in the atria from HS group, and such findings were partially restored by febuxostat and allopurinol treatment. Under the condition of oxidative stress, expressions of Na and Cx40 channels alter, which can contribute to arrhythmogenic electrical remodeling and form AF substrate. Moreover, decreased connexin expression and reduced coupling can contribute to excessive collagen deposition due to enhanced fibroblast activity, leading to increased conduction in homogeneity and proarrhythmia in both atria and ventricles [40]. One possible mechanism of restoration of Cx40 expression by XO inhibitors may be due to direct reduction in oxidative stress in the atria. In addition, mechanical stress is a major contributor to gap junction remodeling through both hypertrophic signal and fibrotic signal [28]. In this study, BP has significantly decreased in Dahl salt-sensitive rats with XO inhibitors, suggesting that a significant reduction in mechanical stress by XO inhibitors might lead to the restoration of gap junction remodeling. Taken together, these results demonstrate that febuxostat and allopurinol attenuate the development of atrial structural and electrical remodeling in Dahl salt-sensitive rats with HS diet.

In the present study, allopurinol was comparably effective for reduction in atrial arrhythmogenic remodeling in hypertensive model, as shown by the previous studies [4,26]. Although febuxostat has been reported to be 1000-fold more potent than allopurinol in the inhibition of ROS or uric acid production by XO in endothelium whereas allopurinol only had a partial effect [43], and although febuxostat was tended to be more effective than allopurinol in suppression of XO activity, CaMKII oxidation, and RyR2 phosphorylation in the present study, there were no significant differences in AF duration between both XO inhibitors. Clinical study is required to determine whether febuxostat or allopurinol has more effective for suppression of AF. In contrast with allopurinol, febuxostat can selectively inhibit XO without cross-inhibiting other enzymes involved in purine and pyrimidine metabolism, and it is better tolerated by patients with renal dysfunction [44] (XO-Kidney, Lin Zhao). We previously reported decreased renal function associated with increased risk for new-onset AF [45]. Recent prospective open-labeled pilot study revealed that febuxostat might not only reduce serum uric acid levels but also suppress plasma renin activity and aldosterone level in hyperuricemic patients with hypertension [46]. Because activated renin-angiotensin aldosterone system plays critical roles in AF pathogenesis by increasing ROS production and CaMKII oxidization, febuxostat could be a potential drug of upstream therapy preventing AF in patients with hypertension and hyperuricemia.

Study limitations

The doses of both XO inhibitors were referred to previous study, and do not try the other dose and treatment duration. In the present study, ERP was measured only at a single site in the LAA, and we did not measure ERP in other parts. Recent meta-analysis of randomized controlled trials of XO inhibitors for prevention of cardiovascular events reported that XO inhibitors did not significantly, but tended to reduce the incidence of adverse cardiovascular events including cardiovascular death, arrhythmia, and stroke [47]. The recent clinical retrospective study showed that febuxostat was associated with higher risk of AF compared with allopurinol in older adults pre-existing CAD [48,49]. The results could not elucidate a reason for the elevated CV risk seen with febuxostat users, they highlight the important of being cognizant that risk does appear to exist; however, the why and to whom remains unclear. Other studied CV endpoints showed no difference between the groups in AF hospitalizations or with CV death, and the risk of heart failure exacerbation was slightly lower in febuxostat initiators [50]. The effect of XO inhibitors on human patients with AF should be verified in clinical setting.

Clinical Science (2021) **135** 2409–2422
https://doi.org/10.1042/CS20210405

Conclusion

The present study provided experimental evidence that XO inhibitors, febuxostat and allopurinol, reduced hypertension-related AF-induced duration and AERP shortening by restoring Ca^{2+} handling pathway and gap junction. XO inhibitors can be an attractive candidate agent of upstream therapy for AF, although further clinical studies are required to establish the evidence.

Clinical perspectives

- AF is the most common sustained arrhythmia, leading to increase in mortality and morbidity, and hypertension is an evident risk factor for AF incidence. Although pulmonary vein isolation has been established as first-line therapy for patients with AF, there is no established preventive therapy.
- The present study demonstrated that XO inhibitors febuxostat reduced hypertension-related AF perpetuation and AERP shortening by restoring Ca^{2+} handling pathway through ox-CaMKII-phosphorylated RyR2 pathway.
- Febuxostat has been clinically used for patients with hyperuricemia, and could be a potential drug of upstream therapy preventing AF in patients with hypertension although further studies are required to establish the clinical evidence.

Data Availability

The authors confirm that the data supporting the findings of the present study are available within the article.

Competing Interests

The authors declare that there are no competing interests associated with the manuscript.

Funding

This work was supported by the MEXT National Institute of Natural Sciences (NINS) [grant number 24790736].

CRediT Author Contribution

DongZhu Xu: Conceptualization, Resources, Data curation, Software, Formal analysis, Supervision, Funding acquisition, Validation, Investigation, Visualization, Methodology, Writing—original draft, Project administration, Writing—review and editing. **Nobuyuki Murakoshi:** Conceptualization, Resources, Data curation, Software, Formal analysis, Supervision, Funding acquisition, Validation, Investigation, Visualization, Methodology, Writing—original draft, Project administration, Writing—review and editing. **Kazuko Tajiri:** Resources, Data curation, Formal analysis, Investigation, Visualization, Methodology. **Feng Duo:** Resources, Data curation, Software, Investigation, Methodology. **Yuta Okabe:** Data curation, Formal analysis, Investigation. **Yoshiko Murakata:** Data curation, Investigation, Methodology. **Zixun Yuan:** Data curation, Software, Investigation, Methodology. **Siqi Li:** Data curation, Investigation, Methodology. **Kazuhiro Aonuma:** Data curation, Investigation, Methodology. **Zonghu Song:** Data curation, Investigation. **Yuzuno Shimoda:** Data curation, Investigation. **Haruka Mori:** Data curation, Investigation, Methodology. **Akira Sato:** Resources, Supervision, Writing—review and editing. **Akihiko Nogami:** Resources, Supervision, Funding acquisition, Writing—review and editing. **Kazutaka Aonuma:** Resources, Supervision, Funding acquisition, Writing—review and editing. **Masaki Ieda:** Resources, Supervision, Funding acquisition, Project administration, Writing—review and editing.

Acknowledgements

The authors thank Mrs.Yumi Isaka for assisting in the experiments.

Abbreviations

AERP, atrial muscle effective refractory period; AF, atrial fibrillation; CaMKII, Ca^{2+}/Calmodulin-dependent kinase II; CL, cycle length; Cx40 , connexin 40; EAD, early after depolarization; EF, ejection fraction; HS, high-salt; LAA, left atrial appendage; LS, low-salt; LV, left ventricular; LVDd, left ventricular diastolic diameter; LVDs, left ventricular systolic diameter; nNOS, neuronal

nitric oxide synthase; ox-CaMKII, oxidized CaMKII; PLB, phospholamban; ROS, reactive oxygen species; RyR2, ryanodine receptor type 2; SERCA, sarcoendoplasmic reticulum Ca2+-ATPase; SBP, systolic blood pressure; XO, xanthine oxidase.

References

1 Benjamin, E.J., Wolf, P.A., D'Agostino, R.B., Silbershatz, H., Kannel, W.B. and Levy, D. (1998) Impact of atrial fibrillation on the risk of death: the Framingham Heart Study. *Circulation* **98**, 946–952, https://doi.org/10.1161/01.CIR.98.10.946
2 Benjamin, E.J., Levy, D., Vaziri, S.M., D'Agostino, R.B., Belanger, A.J. and Wolf, P.A. (1994) Independent risk factors for atrial fibrillation in a population-based cohort. The Framingham Heart Study. *JAMA* **271**, 840–844, https://doi.org/10.1001/jama.1994.03510350050036
3 Mihm, M.J., Yu, F., Carnes, C.A., Reiser, P.J., McCarthy, P.M., Van Wagoner, D.R. et al. (2001) Impaired myofibrillar energetics and oxidative injury during human atrial fibrillation. *Circulation* **104**, 174–180, https://doi.org/10.1161/01.CIR.104.2.174
4 Dudley, Jr, S.C., Hoch, N.E., McCann, L.A., Honeycutt, C., Diamandopoulos, L., Fukai, T. et al. (2005) Atrial fibrillation increases production of superoxide by the left atrium and left atrial appendage: role of the NADPH and xanthine oxidases. *Circulation* **112**, 1266–1273, https://doi.org/10.1161/CIRCULATIONAHA.105.538108
5 Campbell, D.L., Stamler, J.S. and Strauss, H.C. (1996) Redox modulation of L-type calcium channels in ferret ventricular myocytes. Dual mechanism regulation by nitric oxide and S-nitrosothiols. *J. Gen. Physiol.* **108**, 277–293, https://doi.org/10.1085/jgp.108.4.277
6 Wang, Y.G., Rechenmacher, C.E. and Lipsius, S.L. (1998) Nitric oxide signaling mediates stimulation of L-type Ca2+ current elicited by withdrawal of acetylcholine in cat atrial myocytes. *J. Gen. Physiol.* **111**, 113–125, https://doi.org/10.1085/jgp.111.1.113
7 Belevych, A.E., Terentyev, D., Viatchenko-Karpinski, S., Terentyeva, R., Sridhar, A., Nishijima, Y. et al. (2009) Redox modification of ryanodine receptors underlies calcium alternans in a canine model of sudden cardiac death. *Cardiovasc. Res.* **84**, 387–395, https://doi.org/10.1093/cvr/cvp246
8 Greensmith, D.J., Eisner, D.A. and Nirmalan, M. (2010) The effects of hydrogen peroxide on intracellular calcium handling and contractility in the rat ventricular myocyte. *Cell Calcium* **48**, 341–351, https://doi.org/10.1016/j.ceca.2010.10.007
9 Morita, N., Sovari, A.A., Xie, Y., Fishbein, M.C., Mandel, W.J., Garfinkel, A. et al. (2009) Increased susceptibility of aged hearts to ventricular fibrillation during oxidative stress. *Am. J. Physiol. Heart Circ. Physiol.* **297**, H1594–H1605, https://doi.org/10.1152/ajpheart.00579.2009
10 Rokita, A.G. and Anderson, M.E. (2012) New therapeutic targets in cardiology: arrhythmias and Ca2+/calmodulin-dependent kinase II (CaMKII). *Circulation* **126**, 2125–2139, https://doi.org/10.1161/CIRCULATIONAHA.112.124990
11 Purohit, A., Rokita, A.G., Guan, X., Chen, B., Koval, O.M., Voigt, N. et al. (2013) Oxidized Ca(2+)/calmodulin-dependent protein kinase II triggers atrial fibrillation. *Circulation* **128**, 1748–1757, https://doi.org/10.1161/CIRCULATIONAHA.113.003313
12 Erickson, J.R., Joiner, M.L., Guan, X., Kutschke, W., Yang, J., Oddis, C.V. et al. (2008) A dynamic pathway for calcium-independent activation of CaMKII by methionine oxidation. *Cell* **133**, 462–474, https://doi.org/10.1016/j.cell.2008.02.048
13 Neef, S., Dybkova, N., Sossalla, S., Ort, K.R., Fluschnik, N., Neumann, K. et al. (2010) CaMKII-dependent diastolic SR Ca2+ leak and elevated diastolic Ca2+ levels in right atrial myocardium of patients with atrial fibrillation. *Circ. Res.* **106**, 1134–1144, https://doi.org/10.1161/CIRCRESAHA.109.203836
14 Day, R.O., Kamel, B., Kannangara, D.R., Williams, K.M. and Graham, G.G. (2016) Xanthine oxidoreductase and its inhibitors: relevance for gout. *Clin. Sci. (Lond.)* **130**, 2167–2180, https://doi.org/10.1042/CS20160010
15 Ernst, M.E. and Fravel, M.A. (2009) Febuxostat: a selective xanthine-oxidase/xanthine-dehydrogenase inhibitor for the management of hyperuricemia in adults with gout. *Clin. Ther.* **31**, 2503–2518, https://doi.org/10.1016/j.clinthera.2009.11.033
16 Gonzalez, D.R., Treuer, A.V., Castellanos, J., Dulce, R.A. and Hare, J.M. (2010) Impaired S-nitrosylation of the ryanodine receptor caused by xanthine oxidase activity contributes to calcium leak in heart failure. *J. Biol. Chem.* **285**, 28938–28945, https://doi.org/10.1074/jbc.M110.154948
17 Khan, S.A., Lee, K., Minhas, K.M., Gonzalez, D.R., Raju, S.V., Tejani, A.D. et al. (2004) Neuronal nitric oxide synthase negatively regulates xanthine oxidoreductase inhibition of cardiac excitation-contraction coupling. *Proc. Natl. Acad. Sci. U.S.A.* **101**, 15944–15948, https://doi.org/10.1073/pnas.0404136101
18 Tsutsui, H., Kinugawa, S. and Matsushima, S. (2011) Oxidative stress and heart failure. *Am. J. Physiol. Heart Circ. Physiol.* **301**, H2181–H2190, https://doi.org/10.1152/ajpheart.00554.2011
19 Hou, M., Hu, Q., Chen, Y., Zhao, L., Zhang, J. and Bache, R.J. (2006) Acute effects of febuxostat, a nonpurine selective inhibitor of xanthine oxidase, in pacing induced heart failure. *J. Cardiovasc. Pharmacol.* **48**, 255–263, https://doi.org/10.1097/01.fjc.0000249961.61451.da
20 Nomura, J., Busso, N., Ives, A., Matsui, C., Tsujimoto, S., Shirakura, T. et al. (2014) Xanthine oxidase inhibition by febuxostat attenuates experimental atherosclerosis in mice. *Sci. Rep.* **4**, 4554, https://doi.org/10.1038/srep04554
21 Fan, Y.Y., Xu, F., Zhu, C., Cheng, W.K., Li, J., Shan, Z.L. et al. (2019) Effects of febuxostat on atrial remodeling in a rabbit model of atrial fibrillation induced by rapid atrial pacing. *J. Geriatr. Cardiol.* **16**, 540–551
22 Xu, D., Murakoshi, N., Tada, H., Igarashi, M., Sekiguchi, Y. and Aonuma, K. (2010) Age-related increase in atrial fibrillation induced by transvenous catheter-based atrial burst pacing: an in vivo rat model of inducible atrial fibrillation. *J. Cardiovasc. Electrophysiol.* **21**, 88–93, https://doi.org/10.1111/j.1540-8167.2009.01591.x
23 Chen, M., Xu, D., Wu, A.Z., Kranias, E., Lin, S.F., Chen, P.S. et al. (2018) Phospholamban regulates nuclear Ca(2+) stores and inositol 1,4,5-trisphosphate mediated nuclear Ca(2+) cycling in cardiomyocytes. *J. Mol. Cell Cardiol.* **123**, 185–197, https://doi.org/10.1016/j.yjmcc.2018.09.008
24 Wu, A.Z., Xu, D., Yang, N., Lin, S.F., Chen, P.S., Cala, S.E. et al. (2016) Phospholamban is concentrated in the nuclear envelope of cardiomyocytes and involved in perinuclear/nuclear calcium handling. *J. Mol. Cell Cardiol.* **100**, 1–8, https://doi.org/10.1016/j.yjmcc.2016.09.008
25 Xu, D., Murakoshi, N., Igarashi, M., Hirayama, A., Ito, Y., Seo, Y. et al. (2012) PPAR-γ activator pioglitazone prevents age-related atrial fibrillation susceptibility by improving antioxidant capacity and reducing apoptosis in a rat model. *J. Cardiovasc. Electrophysiol.* **23**, 209–217, https://doi.org/10.1111/j.1540-8167.2011.02186.x

Clinical Science (2021) **135** 2409–2422
https://doi.org/10.1042/CS20210405

26 Sakabe, M., Fujiki, A., Sakamoto, T., Nakatani, Y., Mizumaki, K. and Inoue, H. (2012) Xanthine oxidase inhibition prevents atrial fibrillation in a canine model of atrial pacing-induced left ventricular dysfunction. *J. Cardiovasc. Electrophysiol.* **23**, 1130–1135, https://doi.org/10.1111/j.1540-8167.2012.02356.x
27 Yoshizawa, T., Niwano, S., Niwano, H., Tamaki, H., Nakamura, H., Igarashi, T. et al. (2018) Antiremodeling effect of xanthine oxidase inhibition in a canine model of atrial fibrillation. *Int. Heart J.* **59**, 1077–1085, https://doi.org/10.1536/ihj.17-391
28 Shin, S.Y., Jo, W.M., Min, T.J., Kim, B.K., Song, D.H., Hyeon, S.H. et al. (2015) Gap junction remodelling by chronic pressure overload is related to the increased susceptibility to atrial fibrillation in rat heart. *Europace* **17**, 655–663, https://doi.org/10.1093/europace/euu294
29 Kimura, S., Ito, M., Tomita, M., Hoyano, M., Obata, H., Ding, L. et al. (2011) Role of mineralocorticoid receptor on atrial structural remodeling and inducibility of atrial fibrillation in hypertensive rats. *Hypertens. Res.* **34**, 584–591, https://doi.org/10.1038/hr.2010.277
30 Lau, D.H., Shipp, N.J., Kelly, D.J., Thanigaimani, S., Neo, M., Kuklik, P. et al. (2013) Atrial arrhythmia in ageing spontaneously hypertensive rats: unraveling the substrate in hypertension and ageing. *PLoS ONE* **8**, e72416, https://doi.org/10.1371/journal.pone.0072416
31 Korantzopoulos, P., Kolettis, T., Siogas, K. and Goudevenos, J. (2003) Atrial fibrillation and electrical remodeling: the potential role of inflammation and oxidative stress. *Med. Sci. Monit.* **9**, Ra225–Ra229
32 Kim, Y.M., Guzik, T.J., Zhang, Y.H., Zhang, M.H., Kattach, H., Ratnatunga, C. et al. (2005) A myocardial Nox2 containing NAD(P)H oxidase contributes to oxidative stress in human atrial fibrillation. *Circ. Res.* **97**, 629–636, https://doi.org/10.1161/01.RES.0000183735.09871.61
33 Dawson, J. and Walters, M. (2006) Uric acid and xanthine oxidase: future therapeutic targets in the prevention of cardiovascular disease? *Br. J. Clin. Pharmacol.* **62**, 633–644, https://doi.org/10.1111/j.1365-2125.2006.02785.x
34 Christ, T., Boknik, P., Wöhrl, S., Wettwer, E., Graf, E.M., Bosch, R.F. et al. (2004) L-type Ca2+ current downregulation in chronic human atrial fibrillation is associated with increased activity of protein phosphatases. *Circulation* **110**, 2651–2657, https://doi.org/10.1161/01.CIR.0000145659.80212.6A
35 Howe, C.J., Lahair, M.M., McCubrey, J.A. and Franklin, R.A. (2004) Redox regulation of the calcium/calmodulin-dependent protein kinases. *J. Biol. Chem.* **279**, 44573–44581, https://doi.org/10.1074/jbc.M404175200
36 Schulman, H., Hanson, P.I. and Meyer, T. (1992) Decoding calcium signals by multifunctional CaM kinase. *Cell Calcium* **13**, 401–411, https://doi.org/10.1016/0143-4160(92)90053-U
37 Wehrens, X.H. (2011) CaMKII regulation of the cardiac ryanodine receptor and sarcoplasmic reticulum calcium release. *Heart Rhythm* **8**, 323–325, https://doi.org/10.1016/j.hrthm.2010.09.079
38 Nattel, S. (2017) Molecular and cellular mechanisms of atrial fibrosis in atrial fibrillation. *JACC Clin. Electrophysiol.* **3**, 425–435, https://doi.org/10.1016/j.jacep.2017.03.002
39 Gramley, F., Lorenzen, J., Koellensperger, E., Kettering, K., Weiss, C. and Munzel, T. (2010) Atrial fibrosis and atrial fibrillation: the role of the TGF-β1 signaling pathway. *Int. J. Cardiol.* **143**, 405–413, https://doi.org/10.1016/j.ijcard.2009.03.110
40 Tribulova, N., Egan Benova, T., Szeiffova Bacova, B., Viczenczova, C. and Barancik, M. (2015) New aspects of pathogenesis of atrial fibrillation: remodelling of intercalated discs. *J. Physiol. Pharmacol.* **66**, 625–634
41 Davis, L.M., Kanter, H.L., Beyer, E.C. and Saffitz, J.E. (1994) Distinct gap junction protein phenotypes in cardiac tissues with disparate conduction properties. *J. Am. Coll. Cardiol.* **24**, 1124–1132, https://doi.org/10.1016/0735-1097(94)90879-6
42 Chaldoupi, S.M., Loh, P., Hauer, R.N., de Bakker, J.M. and van Rijen, H.V. (2009) The role of connexin40 in atrial fibrillation. *Cardiovasc. Res.* **84**, 15–23, https://doi.org/10.1093/cvr/cvp203
43 Malik, U.Z., Hundley, N.J., Romero, G., Radi, R., Freeman, B.A., Tarpey, M.M. et al. (2011) Febuxostat inhibition of endothelial-bound XO: implications for targeting vascular ROS production. *Free Radic. Biol. Med.* **51**, 179–184, https://doi.org/10.1016/j.freeradbiomed.2011.04.004
44 Zhao, L., Roche, B.M., Wessale, J.L., Kijtawornrat, A., Lolly, J.L., Shemanski, D. et al. (2008) Chronic xanthine oxidase inhibition following myocardial infarction in rabbits: effects of early versus delayed treatment. *Life Sci.* **82**, 495–502, https://doi.org/10.1016/j.lfs.2007.12.010
45 Xu, D., Murakoshi, N., Sairenchi, T., Irie, F., Igarashi, M., Nogami, A. et al. (2015) Anemia and reduced kidney function as risk factors for new onset of atrial fibrillation (from the Ibaraki prefectural health study). *Am. J. Cardiol.* **115**, 328–333, https://doi.org/10.1016/j.amjcard.2014.10.041
46 Tani, S., Nagao, K. and Hirayama, A. (2015) Effect of febuxostat, a xanthine oxidase inhibitor, on cardiovascular risk in hyperuricemic patients with hypertension: a prospective, open-label, pilot study. *Clin. Drug Investig.* **35**, 823–831, https://doi.org/10.1007/s40261-015-0349-8
47 Bredemeier, M., Lopes, L.M., Eisenreich, M.A., Hickmann, S., Bongiorno, G.K., d'Avila, R. et al. (2018) Xanthine oxidase inhibitors for prevention of cardiovascular events: a systematic review and meta-analysis of randomized controlled trials. *BMC Cardiovasc. Disord.* **18**, 24, https://doi.org/10.1186/s12872-018-0757-9
48 Singh, J.A. and Cleveland, J.D. (2019) Comparative effectiveness of allopurinol and febuxostat for the risk of atrial fibrillation in the elderly: a propensity-matched analysis of Medicare claims data. *Eur. Heart J.* **40**, 3046–3054, https://doi.org/10.1093/eurheartj/ehz154
49 Mankad, R. (2019) Cardiovascular safety of febuxostat versus allopurinol in the real world: old reliable comes out on top. *Mayo Clin. Proc.* **94**, 1128–1130, https://doi.org/10.1016/j.mayocp.2019.05.012
50 Zhang, M., Solomon, D.H., Desai, R.J., Kang, E.H., Liu, J., Neogi, T. et al. (2018) Assessment of cardiovascular risk in older patients with gout initiating febuxostat versus allopurinol: population-based cohort study. *Circulation* **138**, 1116–1126, https://doi.org/10.1161/CIRCULATIONAHA.118.033992